ISSN 1990-7931, Russian Journal of Physical Chemistry B, 2019, Vol. 13, No. 2, pp. 383–388. © Pleiades Publishing, Ltd., 2019.
Russian Text © The Author(s), 2019, published in Khimicheskaya Fizika, 2019, Vol. 38, No. 4, pp. 84–90.

CHEMICAL PHYSICS OF NANOMATERIALS

# Optimization of Synthesis of Nanosized Titanium Dioxide Powder Materials from Peroxo Titanium Complex

**E. M. Bayan[a], *, T. G. Lupeiko[a], and L. E. Pustovaya[b]**

[a]*Southern Federal University, Rostov-on-Don, 344006 Russia*
[b]*Don State Federal University, Rostov-on-Don, 344000 Russia*
**e-mail: ekbayan@sfedu.ru*

Received July 13, 2018; revised November 21, 2018; accepted December 20, 2018

**Abstract**—A green-chemistry method of sol–gel synthesis of nanosized titanium dioxide powder materials using a step of the formation of a peroxo titanium complex was optimized. The developed method reduces energy and reactant consumption, rules out the production of toxic wastewater contaminated with organic substances, and improves the environmental performance of the process as a whole. The obtained powder materials are nanosized, and their photocatalytic activity is higher than that of similar materials.

*Keywords:* nanosized materials, titanium dioxide, peroxo titanium complex, wastewater treatment, photo catalysis, green chemistry

**DOI:** 10.1134/S1990793119020131

## INTRODUCTION

Titanium dioxide powder materials constituted by nanosized particles (hereinafter referred to as nanosized powders) are intensely studied in the context of their unique physicochemical properties, first of all, such as photocatalytic and semiconductor ones, etc. [1, 2]. Numerous methods of synthesis of both pure and modified titanium dioxide have been developed [3–7]. It was shown that, by varying the synthesis procedure, the nature of precursors and the medium, the thermal treatment techniques, and other characteristics, one can perform a controlled synthesis of a material with preset properties. The totality of experimental data currently allows one to consider the environmental performance of the main proposed synthesis methods and their material and energy consumption and determine the optimal method for manufacturing nanosized materials based on titanium dioxide.

In view of this, we proposed to optimize the method for producing photocatalytically active titanium dioxide from a peroxo titanium complex (PTC) with the widely used sol–gel technology, pursuant to the basic principles of green chemistry [8]. This complex is actively used as a precursor because it makes it possible to obtain a finely divided nanosized titanium dioxide powder owing to the electrostatic repulsion of likely charged peroxide groups sorbed on the surface of the gel, which prevent agglomeration in solution to form larger micelles [9, 10]. PTC has been successfully used to produce not only classical nanosized powder materials with spherical morphology in the anatase modification [11] but also nanosized semiconductor films [12–15] and composites [16–19], as well as powdered materials comprising particles shaped as hollow spheres [20], dodecahedra [21], and nanosized ellipsoids [9, 22].

It is known that the initial reactants for synthesis of nanosized titanium dioxide from PTC can be either organic [23, 24] or inorganic [25] Ti(IV) derivatives with subsequent treatment of titanium hydroxide with hydrogen peroxide. It was shown that finely divided materials are obtained at low temperatures of precipitation from diluted solutions of Ti(IV) derivatives [26]. The acidity of the medium largely determines the structure of the material. For example, the anatase modification forms at pH 6–7; the rutile modification, at pH 0; and the brookite one, at pH 1 [26, 27]. A nanosized titanium dioxide powder is most often produced by hydrothermal and thermal treatment [12–27]. Analyzing this pathway of synthesis in the context of its compliance with the main principles of green chemistry [8], one can conclude that it is energy-intensive and results in the production of wastewater containing significant amounts of various toxic organic contaminants.

In this work, we presented the results of the optimization of the method for synthesizing photocatalytically active nanosized titanium dioxide powder materials by the sol–gel technology in which organic precursors are placed by inorganic ones and an energy-intensive step of the synthesis is eliminated without sacrificing the characteristics of the end product.

## SYNTHESIS OF MATERIALS

The initial reactant of the sol–gel synthesis was titanium tetrachloride (chemically pure), a titanium-containing inorganic precursor, because it was shown [27] that the nature of the anion of a precursor has no significant effect on the phase formation of titanium dioxide if it is synthesized through PTC. The choice of an inorganic precursor makes it possible to eliminate toxic organic substances from the synthesis, thus improving the environmental performance of the process. Also, in the synthesis in this work, we conventionally selected 25% aqueous ammonia solution (analytically pure) as a precipitant, 30% aqueous $H_2O_2$ solution (chemically pure), and distilled water.

Primarily, from titanium tetrachloride, at a temperature of 0–5°C, a solution with a titanium content of $[Ti^{4+}] = 0.1$ M was obtained. By enhancing the hydrolysis of the aqueous solution containing $Ti^{4+}$ ions by adding the ammonia solution, a white amorphous gel of oxo and hydroxo compounds of titanium was synthesized, which was conditionally called titanium hydroxide. Because the effect of the acidity of the medium on the properties of the gel was previously [26, 27] studied in detail when the pH of the precipitation medium was in the range 0–7, in this work, we restricted our investigation of the effect of this factor to the pH range 7–14. The produced gel was filtered off and washed with distilled water to remove impurity ions (ammonium cations and chloride anions). The residual $Cl^-$ content in water after filtration early in the washing was tested by a qualitative reaction with a silver nitrate solution. In the absence of turbidity, quantitative colorimetric determination of chlorides was performed [28]. At this step of the synthesis, the maximum possible amount of impurity ions is removed, which guarantees the purity of the obtained product.

Further, with the addition of the 30% aqueous hydrogen peroxide solution to titanium hydroxide while stirring, PTC was synthesized. The pattern of the process changed with time: initially, a yellow colloidal solution formed, and in an hour, the solution became transparent and yellow-orange in color.

It is known [29] that $O_2^{2-}$ peroxide ions interact with solutions of titanyl salts to form various peroxo titanium complexes of characteristic color, the value and intensity of which depend on the acidity of the medium. The color of the solutions may vary from orange-red in a strongly acidic medium to yellow in the transition to a neutral medium.

The PTC we synthesized was held for several hours at 20°C to complete the decomposition of the excess of hydrogen peroxide. Then, the solution with PTC was treated on a water bath until the formation of a transparent yellow xerogel, which was stable in air for more than 10 days.

Most of the researchers who used PTC as a precursor carried out further titanium dioxide synthesis using various variants of hydrothermal treatment [12–27], which is an extremely energy-intensive and low-efficiency step; it can be justified only by the need to produce particles with strictly determined morphology. Hydrothermal treatment has no essential influence on photocatalytic properties. Therefore, to increase the energy efficiency of the titanium dioxide production technology, we conducted this process in two less energy-intensive steps. The first step was isothermal treatment for 12 h at 100°C, during which the xerogel decomposed to form a white powder. At the second stage, the obtained intermediate product was ground and then annealed for 2 h at a given temperature. For comparison, we synthesized materials based on titanium dioxide without PTC production step. Table 1 presents the main synthesis parameters and properties of the obtained materials.

## METHODS OF INVESTIGATION

The phase formation in the synthesis of the $TiO_2$-based nanomaterials was studied by differential scanning calorimetry and thermogravimetric analysis with an STA 449°C/4 G Jupiter Jupted synchronous thermal analyzer (Germany) during heating in air from 293 to 1173 K at a rate of 10 deg/min.

The X-ray powder diffraction analysis was carried out with an ARL X'TRA powder diffractometer (Thermo ARL, Switzerland) in Cu$K_\alpha$ radiation. The sizes of coherent scattering domains (CSD) were calculated from the change in the shape of the diffraction reflection profile according to the Debye–Scherrer equation [30]. The morphology of the samples was observed by transmission electron microscopy with a Tecnai G2 Spirit Bio TWIN transmission electron microscope. Solid-phase samples of the nanosized materials were investigated by IR spectroscopy with an FSM 1202 FTIR spectrometer in the range 500–4000 $cm^{-1}$.

The photocatalytic activity of the obtained samples was studied using a model reaction of photodegradation of the organic dye methylene blue $C_{16}H_{18}ClN_3S$ in aqueous suspensions of titanium dioxide under UV radiation (at a wavelength of more than 380 nm). This organic substance was chosen as a model contaminant because its molecule contains cycles that are quite difficult to break, along with sulfur, nitrogen, and chlorine. This is an organic substance of the cationic type. Its catalytic decomposition can be described by the equation

$$2C_{16}H_{18}ClN_3S + 51O_2 = 2HCl + 2H_2SO_4 + 6HNO_3 + 32CO_2 + 12H_2O.$$

The residual concentration of methylene blue was determined spectrophotometrically using a calibration curve with a YuNIKO 1201 spectrophotometer. To estimate the photocatalytic activity from the obtained data, the fraction $C/C_0$ of the remaining methylene blue in the solution was calculated.

**Table 1.** Parameters of synthesis and materials

| No. of sample | Type of complex ion | pH of precipitation | Heat treatment | | Average powder particle size, nm | |
|---|---|---|---|---|---|---|
| | | | $T$, °C | time, h | CSD | TEM |
| 1 | Aqua | 7 | 100 | 24 | 15 | 17 |
| 2 | Aqua | 7 | 500 | 2 | 20 | 19 |
| 3 | Aqua | 7 | 600 | 2 | 22 | 21 |
| 4 | Aqua | 14 | 600 | 2 | 31 | 28 |
| 5 | Aqua | 7 | 700 | 2 | 26 | 26 |
| 6 | Peroxo | 7 | 100 | 24 | 10 | 9 |
| 7 | Peroxo | 7 | 400 | 2 | 11 | 10 |
| 8 | Peroxo | 7 | 500 | 2 | 14 | 12 |
| 9 | Peroxo | 7 | 600 | 2 | 22 | 20 |
| 10 | Peroxo | 7 | 700 | 2 | 25 | 23 |
| 11 | Peroxo | 14 | 500 | 2 | 13 | 11 |
| 12 | Peroxo | 14 | 600 | 2 | 14 | 13 |

## RESULTS AND DISCUSSION

The presence of residual peroxo groups in the amorphous titanium dioxide powders synthesized from the PTC gel and dried at 100°C was checked by IR spectroscopy. The characteristic stretching vibrations of the peroxo group at 894 $cm^{-1}$ are absent. The wide absorption band at 3200–3500 $cm^{-1}$ indicates the presence of $OH^-$ groups in all the studied samples. Hydroxyl groups can either belong to water molecules or be coordinated by titanium. Moreover, at 500–700 $cm^{-1}$, vibrations of titanium–oxygen bonds in $[TiO_6]$ octahedra are observed.

The data of the thermal and thermogravimetric analyses of the samples have the form conventional for materials of this type (Fig. 1). The shape of the thermogravimetric analysis curve shows that the process occurs in several steps. The endothermic peak at 100°C characterizes the phase transformation of water into vapor and the removal of the vapor from the system. In the temperature range 20–400°C, there is a total loss of the weight of the sample (26%), which is due to the decomposition of the titanium-containing compound to form titanium dioxide. The diffuse exothermic peak in the range 200–370°C is induced by the formation of a polycrystalline nanosized anatase phase, which agrees with the X-ray powder diffraction analysis data (Fig. 2). At temperatures above 400°C, the weight of the sample stabilizes, and thermal events due to the formation of new phases are not observed. Based on the obtained data, the annealing temperatures were chosen to be 500 and 600°C.

Figure 2 presents the X-ray powder diffraction patterns of the nanomaterials based on titanium dioxide. The initial (nonannealed) samples are conventionally X-ray amorphous (Fig. 2, curve *1*). In annealing, all the materials crystallize in the anatase modification of titanium dioxide before 700°C. No peaks of a rutile or brookite phase were detected, which demonstrates the high purity of the products. It is noteworthy that if a preliminary boiling of the PTC gel is included, then, even at 600°C. an impurity phase of titanium dioxide in the rutile modification forms, which reduces the photocatalytic properties of the material [23]. With increasing heat-treatment temperature, the particles grow, which leads to an increase in the intensity of peaks and a decrease in their full widths at half maxima. A comparison of the X-ray powder diffraction patterns of the materials obtained without the step of the formation of PTC and through the formation of PTC and treated under the same temperatures shows that the sizes of particles of the powder materials produced by the proposed optimized sol–gel method are smaller (Fig. 2).

In numerous works, the significance of the pH of the titanium hydroxide precipitation medium was determined [26, 27, 31]. Oxo and hydroxotitanates are

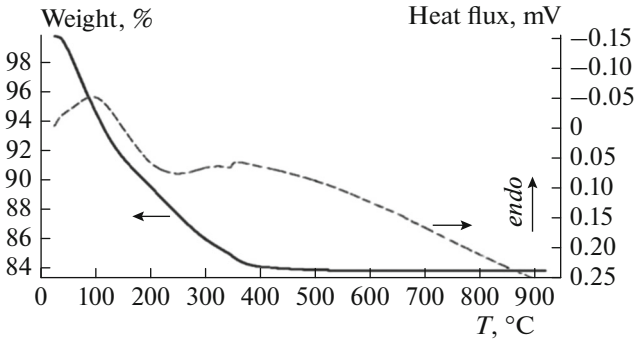


**Fig. 1.** Data on the thermogravimetric derivatographic analysis of the material obtained through the step of the formation of PTC.

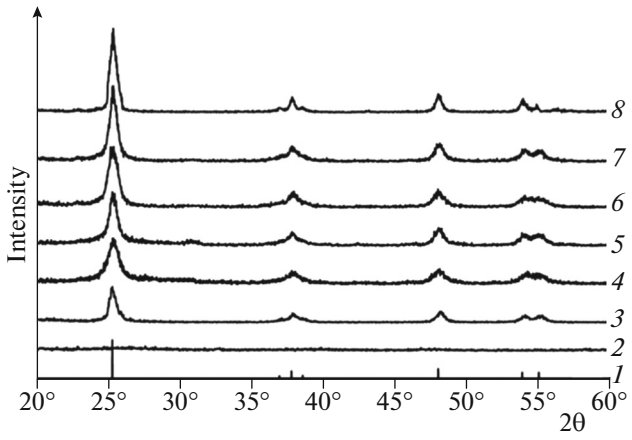


**Fig. 2.** X-ray powder diffraction patterns of (*1*) anatase from database and (*2*) the nanosized materials produced by the sol–gel method (*2*–*5*) through the step of the formation of PTC and (*6*–*8*) without this step and annealed at (*3*, *6*) 500, (*4*, *7*) 600, and (*5*, *8*) 700°C.

known to incompletely precipitate in acidic and weakly acidic media. We showed that the pH 7 of the precipitation medium ensures the optimal combination of such requirements that complete precipitation, single-phase medium, nanosized particles, high catalytic activity, and low precipitant consumption.

The average sizes of crystallites in the nanosized materials synthesized from PTC (Table 1) that were calculated by the Debye–Scherrer equation at the peak of anatase (101) range from 13 to 22 nm. The particle sizes in the reference samples produced without the stage of the formation of PTC are somewhat larger: from 22 to 31 nm.

The size and morphology of particles of the nanosized materials were also analyzed by transmission electron microscopy. It was shown that the materials synthesized from PTC are characterized by a near-spherical shape of particles. The materials are quite uniform, with an average particle size of 15–20 nm (Fig. 3). This result agrees with the data calculated from the results of the X-ray powder diffraction analysis.

Figure 4 illustrates the photodegradation of methylene blue on the synthesized materials. Material no. 9 (Table 1) obtained from PTC and annealed at 600°C has the highest photocatalytic activity, which exceeds the photocatalytic activity of a commercial sample of Degussa P25 (a mixture of two $TIO_2$ phases: anatase and rutile). Figure 4 also shows that reference samples no. 1–3 have almost no photocatalytic activity.

In studying the effect of the pH of the precipitation medium on the photocatalytic properties of the obtained materials, it was found that the highest photocatalytic activity was demonstrated by materials no. 8–10 (Table 1), which were synthesized at pH 7

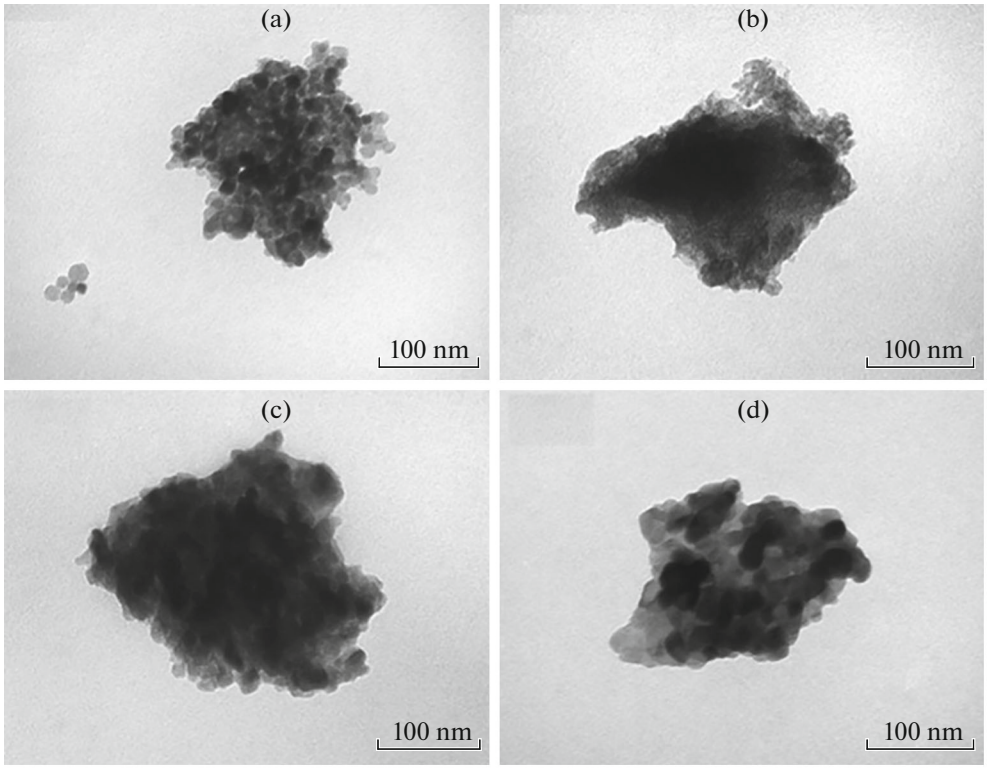


**Fig. 3.** Transmission electron spectroscopy images of the materials synthesized from PTC at the following pH and temperatures of the medium: (a) pH 7 and 500°C, (b) pH 7 and 600°C, (c) pH 14 and 500°C, and (d) pH 14 and 600°C.

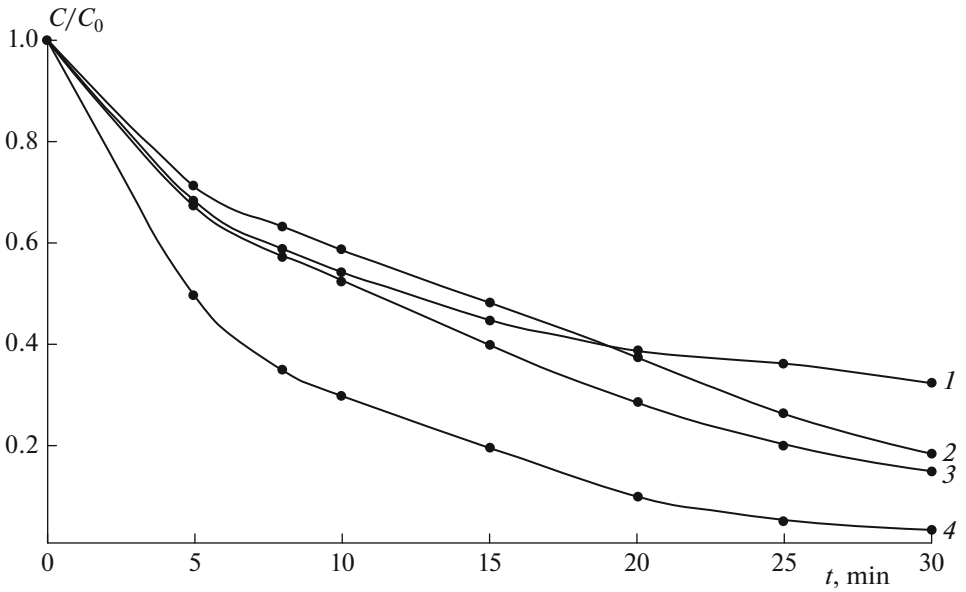


**Fig. 4.** Photodegradation of methylene blue on Degussa P25 (curve *1*) and on the materials obtained from the reference sample of titanium dioxide (curve *4*, sample no. 3) and peroxo titanium complex (curve *2*, sample no. 9; curve *3*, sample no. 8) at pH 7, annealed at 600°C (curve *2*, sample no. 9; curve *4*, sample no. 3) and 500°C (curve *3*, sample no. 8).

(Fig. 4). Materials no. 4, 11, and 12, which were obtained at pH 14, have low photocatalytic activity, probably because of the blocking of the surface of the heterogeneous catalyst by inactive impurities because of the high sorption activity of the material.

Thus, the $TiO_2$-based nanosized materials synthesized from PTC have high photocatalytic activity, which enables one to recommend them as efficient catalysts for removing organic contaminants from water. This method of synthesis is compliant with the main principles of green chemistry, has a high product yield owing to the completeness of precipitation, and low energy consumption, thanks to elimination of hydrothermal treatment. The reactants in this method do not include toxic organic reagents. Thus, the proposed synthesis method is simple, cost-effective, and environmentally friendly.

## ACKNOWLEDGMENTS

We thank the "Modern Microscopy" Center for Shared Use of Scientific Equipment, Southern Federal University, Rostov-on-Don, Russia, for allowing us to study the microstructure of the samples.

## REFERENCES

1. R. C. Thompson, Phys. Inorg. Chem. **15** (38), 1 (1984). https://doi.org/10.1002/chin.198438031
2. M. V. Shankar, T. Kako, D. Wang, and J. Ye, J. Colloid Interface Sci. **331**, 132 (2009).
3. E. M. Bayan, T. G. Lupeiko, E. V. Kolupaeva, et al., in *Advanced Materials – Techniques, Physics, Mechanics and Applications,* Vol. 193 of *Springer Proceedings in Physics,* Ed. by I. A. Parinov, Chang Shun-Hsyung, and M. A. Jani (Springer, Heidelberg, New York, Dordrecht, London, 2017), p. 17. https://doi.org/10.1007/978-3-319-56062-5_2
4. Y. Zhang, J. Bai, L. Zhou, et al., J. Colloid Interface Sci. **536**, 215 (2019).
5. E. M. Bayan, T. G. Lupeiko, L. E. Pustovaya, A. A. Knyashchuk, and A. G. Fedorenko, Russ. J. Phys. Chem. B **11**, 600 (2017). https://doi.org/10.1134/S1990793117040042
6. M. Hamadanian, S. Karimzadeh, V. Jabbari, and D. Villagrán, Mater. Sci. Semicond. Process. **41**, 168 (2016). https://doi.org/10.1016/j.mssp.2015.06.085
7. M. Crişan, N. Drâgan, D. Crişan, A. Ianculescu, et al., Ceram. Int. **42**, 3088 (2016). https://doi.org/10.1016/j.ceramint.2015.10.097
8. P. T. Anastas and J. C. Warner, *Green Chemistry: Theory and Practice* (New York, Oxford Univ. Press, 1998).
9. G. S. Zakharova and E. I. Andreikov, Inorg. Mater. **48**, 727 (2012).
10. S. Wang, H. Yu, Sh. Yuan, and L. Shi, Res. Chem. Intermed. **42**, 3775 (2016). https://doi.org/10.1007/s11164-015-2244-6
11. E. M. Bayan, T. G. Lupeiko, L. E. Pustovaya, and A. G. Fedorenko, Nanotechnol. Russ. **12**, 269 (2017). https://doi.org/10.1134/S199507801703003X
12. Y. Miao and J. Gao, J. Solid State Chem. **196**, 372 (2012).
13. N. S. Shabanov, A. Sh. Asvarov, A. Chioleriod, et al., J. Colloid Interface Sci. **498**, 306 (2017). https://doi.org/10.1016/j.jcis.2017.03.075
14. Y. Li, Y. Yu, L. Wu, and J. Zhi, Appl. Surf. Sci. **273**, 135 (2013). https://doi.org/10.1016/j.apsusc.2013.01.213

15. R. Zhang, Y. Zhang, C. Xu, et al., Proc. SPIE **8409**, 84092 (2012). https://doi.org/10.1117/12.922192
16. R. Morozov, I. Krivtsova, V. Avdin, et al., J. Non-Cryst. Solids **435**, 8 (2016). http://doi.org/10.1016/j.jnoncrysol.2015.12.024
17. Q. Zhao, W. Wen, Y. Xia, and J. Wu, Thin Solid Films **648**, 103 (2018). https://doi.org/10.1016/j.tsf.2018.01.004
18. W. Low and V. Boonamnuayvitaya, Mater. Res. Bull. **48**, 2809 (2013). http://doi.org/10.1016/j.materresbull.2013.04.020
19. M. Ilkaeva, I. Krivtsov, V. Avdin, et al., Colloids Surf., A **456**, 120 (2014).
20. D. Wu, F. Zhu, J. Li, and D. Xu, J. Mater. Chem. **22**, 11665 (2012). https://doi.org/10.1039/C2JM30786C
21. N. Murakami, S. Kawakami, T. Tsubota, and T. Ohno, J. Mol. Catal. A: Chem. **358**, 106 (2012). https://doi.org/10.1016/j.molcata.2012.03.003
22. Y. Zhang, L. Wu, Q. Zeng, and J. Zhi, Mater. Chem. Phys. **121**, 235 (2010). https://doi.org/10.1016/j.matchemphys.2010.01.024
23. Y. Liu, M. Aizawa, Z. Wang, et al., J. Colloid Interface Sci. **322**, 497 (2008). https://doi.org/10.1016/j.jcis.2008.03.034
24. X. Bao, S. Yan, F. Chen, and J. Zhang, Mater. Lett. **59**, 412 (2005).
25. D. Nguyen, W. Wang, H. Long, and H. RU, Front. Mater. Sci. **10**, 23 (2016). https://doi.org/10.1007/s11706-016-0322-3
26. Y. Zhang, L. Wu, Q. Zeng, and J. Zhi, J. Phys. Chem. C **112**, 16457 (2008). https://doi.org/10.1021/jp804524y
27. S. I. Seok, M. Vithal, and J. A. Chang, J. Colloid Interface Sci. **346**, 66 (2010). https://doi.org/10.1016/j.jcis.2010.02.049
28. M. O. Gorbunova, E. M. Bayan, A. V. Shevchenko, and M. S. Kulyaginova, Anal. Kontrol'. **21**, 274 (2017). https://doi.org/10.15826/analitika.2017.21.3.007
29. Yu. D. Tretyakov, *Inorganic Chemistry* (Akademiya, Moscow, 2007), Vol. 3 [in Russian].
30. V. Stengl, S. Bakardjieva, and N. Murafa, Mater. Chem. Phys. **114**, 217 (2009). https://doi.org/10.1016/j.matchemphys.2008.09.025
31. E. M. Bayan, T. G. Lupeiko, L. E. Pustovaya, and A. G. Fedorenko, in *Advanced Materials Manufacturing, Physics, Mechanics and Applications,* Vol. 175 of *Springer Proceedings in Physics,* Ed. by I. A. Parinov, Shun-Hsyung Chang, and V. Yu. Topolov (Springer, Heidelberg, New York, Dordrecht, London, 2016), p. 51. https://doi.org/10.1007/978-3-319-26324-3_4

*Translated by V. Glyanchenko*